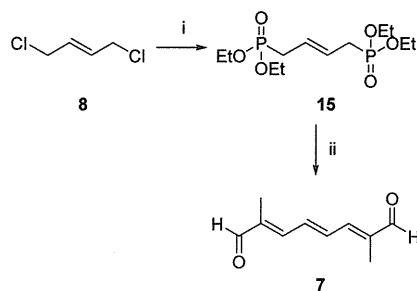
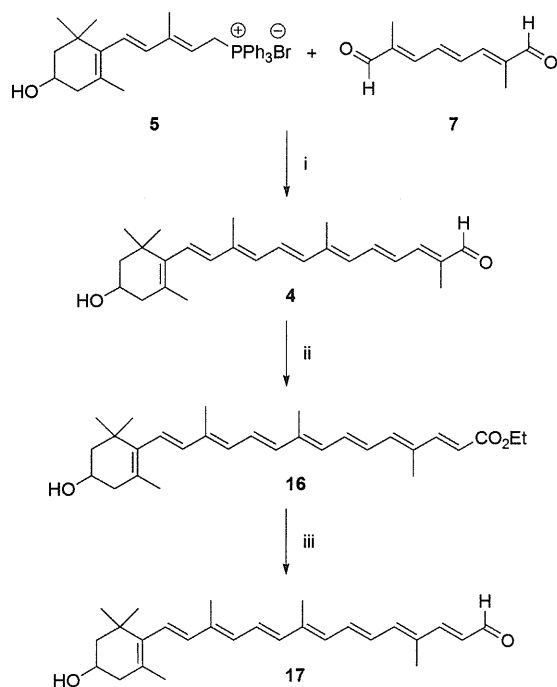


Scheme 3. Synthesis of C_{10} -Dialdehyde **7**^a

^aReagents and conditions: (i) $P(OEt)_3$, 0.4 MPa, 160 °C, 2 h, 92% yield; (ii) $MeCOCH(OMe)_2$, NaH, THF, 0 to 60 °C, 3 h, then 20% aqueous H_2SO_4 , 0 to 50 °C, 2.5 h, 35% yield over two steps.

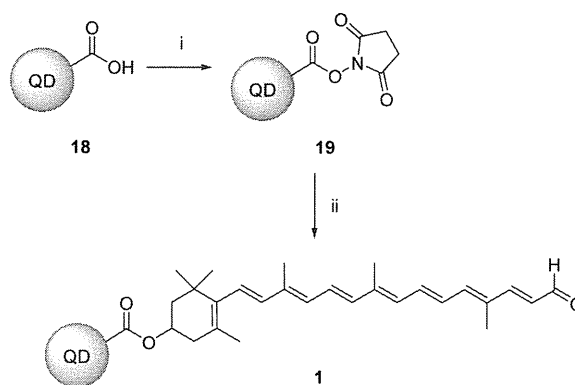
dimethyl acetal under the basic conditions afforded the desired C_{10} -dialdehyde **7** in 35% yield over two steps.

The Wittig olefination of C_{15} -phosphonium ylide **5** with C_{10} -dialdehyde **7** was initiated by adding 1,2-epoxybutane to successfully afford C_{25} -aldehyde **4** in 58% yield. The treatment of C_{25} -aldehyde **4** with carbethoxymethylene triphenylphosphorane afforded ester **16**, which was reduced with DIBAL followed by oxidation with manganese dioxide to afford the desired C_{27} -aldehyde **17** in 44% yield over two steps (Scheme 4).

Scheme 4. Synthesis of C_{27} -Aldehyde **17**^a

^aReagents and conditions: (i) 1,2-epoxybutane, reflux, overnight, 58% yield; (ii) $Ph_3P=CHCOOEt$, THF, 90 °C, 7 h; (iii) DIBAL, Et_2O , 0 °C, 30 min, then MnO_2 , CH_2Cl_2 , 0 °C, 3.5 h, 44% yield over two steps.

The critical step was the coupling of commercially available and colloidal carboxyl QD (QD-COOH, **18**)¹¹ to C_{27} -aldehyde **17** via an ester bond formation (Scheme 5).¹² First, the carboxylic acid group of **18** was activated by preparing the corresponding *N*-hydroxysuccinimide (NHS) ester **19** in the presence of 1-(3-(dimethylamino)propyl)-3-ethylcarbodiimide

Scheme 5. Coupling Reaction of QD to C_{27} -Aldehyde **17**^a

^aReagents and conditions: (i) EDC, NHS, MES buffer; (ii) **17**, DMF, 24 h.

hydrochloride (EDC, 1,000 equiv) and NHS (1,000 equiv) in 2-(*N*-morpholino)ethanesulfonic acid buffer (MES) at pH 6. Then, ester **19** was reacted with C_{27} -aldehyde **17** (100 equiv) in DMF for 24 h to afford conjugate **1**.

The formation of conjugate **1** was confirmed by measuring its fluorescence spectrum to observe the change in the maximum wavelength of the reaction mixture compared to that of QD-COOH **18** and C_{27} -aldehyde **17**. The fluorescent nanocrystal QD 510 used in this study with a CdTe core is hydrophilic owing to the COOH groups on its surface. The molar weight of the nanocrystal is approximately 3000. The absorption spectrum shows that QD 510 absorbs energy across a broad range of the spectrum; therefore, it can be excited at different wavelengths. The QD 510 emits sharply with a defined narrow emission peak at 515 nm in DMSO (Figure 2, the absorption and fluorescence spectra are normalized). The sample was also excited at 460 nm that is the maximum wavelength for absorption of C_{27} -aldehyde **17** in DMSO.

The absorption of C_{27} -aldehyde **17** shows a low degree of resolution in its vibronic bands because of the presence of one bulky isoprenoid ring coupled to the conjugated π -electrons in the double-bond chain, thereby increasing the conformational disorder in the polyene chain. The fluorescence spectrum of C_{27} -aldehyde **17** was thought to be composed of two

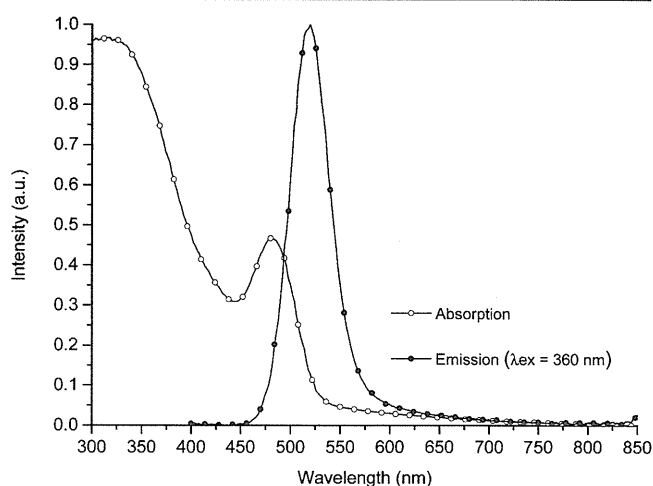


Figure 2. Room-temperature absorption and fluorescence spectra of QD 510 in DMSO.

components, centered at 585 and 768 nm (Figure 3). Moreover, the excitation-wavelength dependence of the

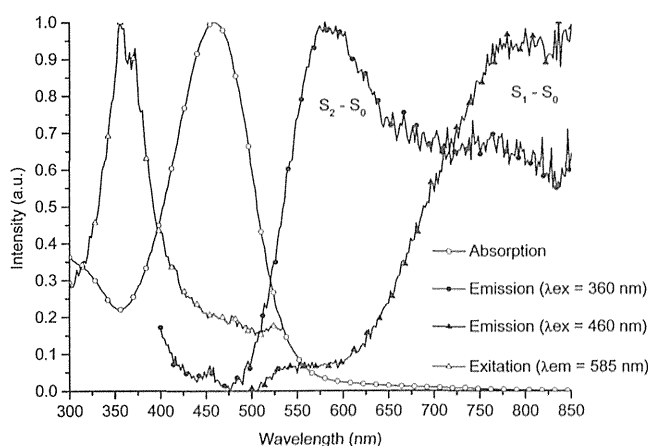


Figure 3. Room-temperature absorption and fluorescence spectra of C_{27} -aldehyde 17 in DMSO.

fluorescence spectrum of C_{27} -aldehyde 17 in DMSO was carefully examined. It was found that the intensity of the short-wavelength band at 585 nm fluorescence decreases with increasing excitation wavelength. This behavior was accompanied by an increase in the long-wavelength emission band centered at 768 nm.

The change in the fluorescence of the reaction mixture with time was also examined (Figures 4 and 5). The reaction was

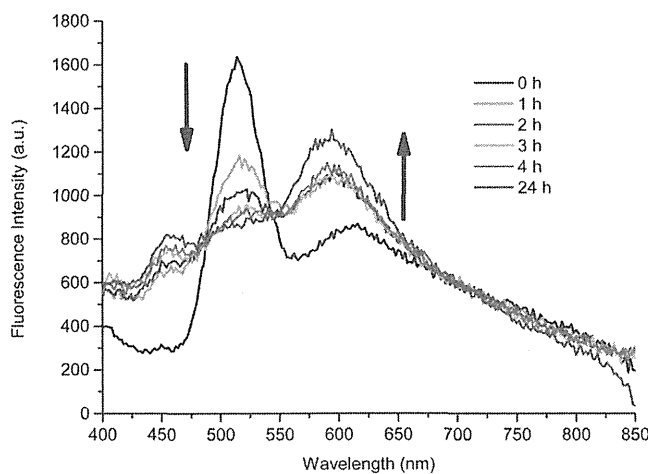


Figure 4. Fluorescence spectra of the reaction mixture in DMSO with time ($\lambda_{ex} = 360$ nm).

performed in the presence of EDC and NHS in MES buffer for 24 h. The results showed that in DMSO, the fluorescence intensity centered at 515 nm decreased with the increase in the intensity at 595 nm, which is close to the maximum wavelength of C_{27} -aldehyde 17 in DMSO (585 nm). For further evidence, the coupling reaction in different solvent systems was also investigated. The maximum fluorescence wavelength in DMF blue-shifted to 573 nm compared to 595 nm in DMSO because of the solvent effect.

The fluorescence spectra of the reaction mixture showed a change in the maximum fluorescence wavelength from 515 nm for the QD to 595 nm for the reaction mixture, which is close to that of C_{27} -aldehyde 17 in DMSO centered at 585 nm.

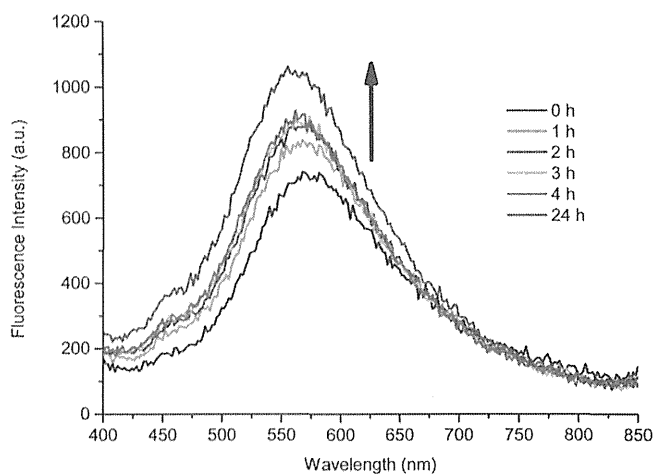


Figure 5. Fluorescence spectra of the reaction mixture in DMF with time ($\lambda_{ex} = 355$ nm).

Furthermore, the fluorescence intensity was found to increase with the progress of the reaction. The results remarkably showed the occurrence of fluorescence resonance energy transfer (FRET, Figure 6), in which the QD acts as the

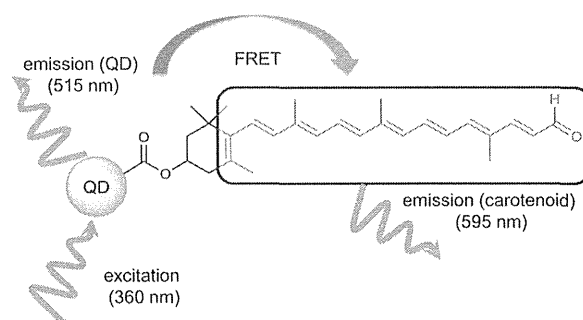


Figure 6. Energy transfer from QD to carotenal in DMSO.

donor fluorophore and transfers the excited energy to the C_{27} -aldehyde moiety that acts as the acceptor chromophore. The fluorescence measurement with time showed the same result as that in DMF; the fluorescence intensity of the band centered at 510 nm decreased with increasing intensity at 573 nm, which is close to the maximum wavelength of C_{27} -aldehyde 17 in DMF (565 nm). Once more, it confirms the radiationless transmission of energy from a donor molecule to an acceptor molecule. The transfer of energy leads to a decrease in the donor fluorescence intensity and excited-state lifetime and an increase in the acceptor's emission intensity.

There is a slow decrease in the fluorescence intensity at 515 nm in DMSO, which was not observed in DMF, indicating that the reaction rate in DMF was faster than that in DMSO. Although the rate of reaction in DMF is faster, DMSO should be used for this reaction because of its lower toxicity for the plant cells. DMSO has a low acute and chronic toxicity in animal, plant, and aquatic life, and it has been applied widely for cell introduction.

A concentration-dependent fluorescence intensity was examined under the same coupling reaction conditions of QD 510 with different equivalents of C_{27} -aldehyde 17 (70, 90, and 100 equiv) in DMSO. The reaction was stirred for 1 h, and the fluorescence spectra were recorded. The results clearly indicated that there is a decrease in the fluorescence intensity at

515 nm and an increase at 595 nm (Figure 7). The number of carotenal moieties bound to QD increased with the increasing

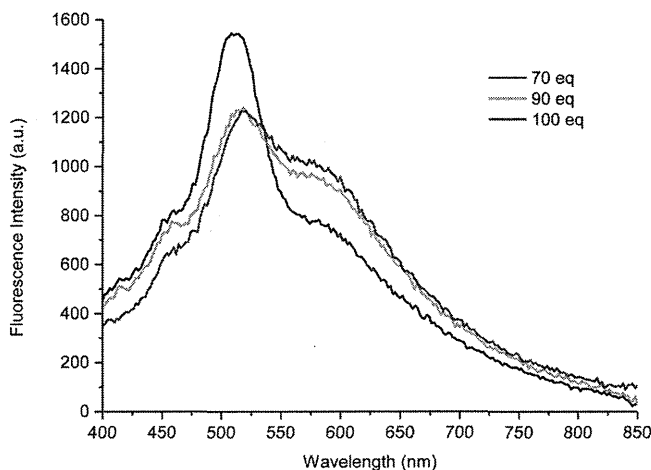


Figure 7. Concentration-dependent fluorescence intensity at different contraction ($\lambda_{\text{ex}} = 360$ nm, the reactions were performed for 1 h).

equivalence of C_{27} -aldehyde 17. This leads to the change in the intensities of the peaks at 515 and 595 nm with the change in concentration of C_{27} -aldehyde 17.

To investigate whether the nonspecific adsorption of the carotenal moiety occurred on the QD surface, the control experiments were carried out using the same coupling procedure for QD 510 and C_{27} -aldehyde 17 in DMF and DMSO in the absence of EDC and NHS in MES buffer. The results of the fluorescence measurements strongly showed that the photophysical properties of QD 510 remained unchanged; however, no characteristic bands of the carotenal moiety were detected in the emission spectra (Figure 8). The blank

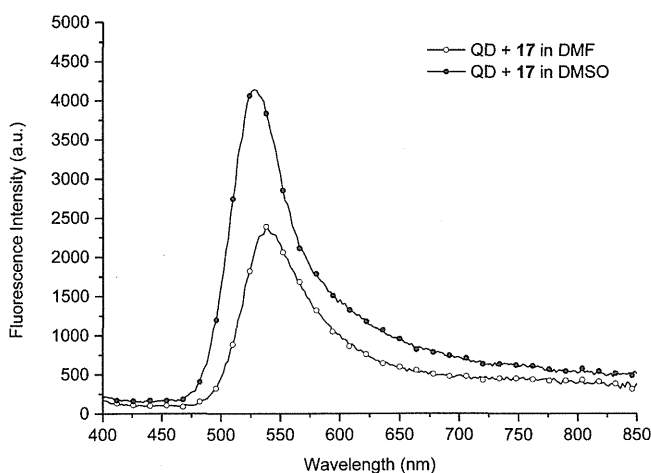


Figure 8. Fluorescence spectra of reaction between QD 510 and C_{27} -aldehyde 17 in DMF (○) and DMSO (●) in the absence of coupling reagents.

experiment showed that the signal observed in the case of apocarotenal–QD conjugate 1 is not because of the nonspecific adsorption of the dye; it is attributed to the expected covalent linking of apocarotenal to QD.

To explore potential changes in living plants the temperature-, light-, and pH-dependence of QD 510 nm was measured in an aqueous environment. At room temperature we observed

no changes in the fluorescence emission. At 30 °C after 3 h, at 70 °C, and at low pH values of 5 we determined small shifts in the maximum wavelengths (See Supporting Information [SI]). Even if such extremes were to occur in our *in vivo* experiments, these variations would still enable us to determine the FRET phenomena, where we found a shift of the maximum wavelength from 515 to 595 nm (Figure 4).

The fluorescence emission spectrum of the donor QD molecule overlaps with the absorption spectrum of the acceptor carotenoid molecule, and the two are within a minimal spatial radius in the range 10–100 Å; therefore, the donor molecule can directly transfer its excitation energy to the acceptor molecule through long-range dipole–dipole intermolecular coupling (Figures 6 and 9). For the detailed investigation of

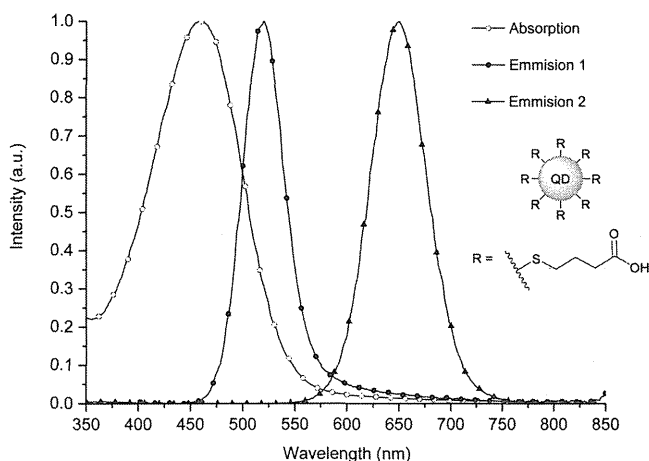


Figure 9. Absorption of C_{27} -aldehyde 17 (○) and fluorescence of reaction mixture with QD 510 (●) and QD 620 (▲) in DMSO ($\lambda_{\text{ex}} = 360$ nm).

the methodology, the EDC-mediated coupling reaction was repeated using a different QD: (CdTe) 620.¹¹ The fluorescence emission intensity of the reaction mixture at 630 nm (excited at 360 nm) after 24 h remained unchanged in DMSO (Figure 9). This clearly demonstrates that there is no FRET between QD 620 and the apocarotenal moiety because of no overlap between the absorption of apocarotenal and the emission spectra of QDs.

Commercially available QD (CdSe/ZnS) 525 and 625 were also examined for the coupling reaction.¹³ The fluorescence of the reaction mixture after coupling for 24 h showed the maximum intensities at 530 and 630 nm for QD (CdSe/ZnS) 525 and 625, respectively; no change in the fluorescence was observed (Figure 10). The slight red shift can be attributed to the solvent effect. Although the absorption of apocarotenal overlapped with the fluorescence of QD 525, the FRET did not occur. This is probably because of the small overlapping area and different structure of QD 525, i.e., the core–shell material of this nanocrystal is further coated with another polymer layer. Therefore, it increased the distance between the QD and apocarotenal.

Finally, in preliminary experiments we could confirm the uptake of the reaction mixture with QD 510 in *Arapdosopsis* seedlings by means of confocal laser microscopy (See SI).

CONCLUSION

We reported the design and synthesis of apocarotenal–QD conjugate 1. To the best of our knowledge, this is the first

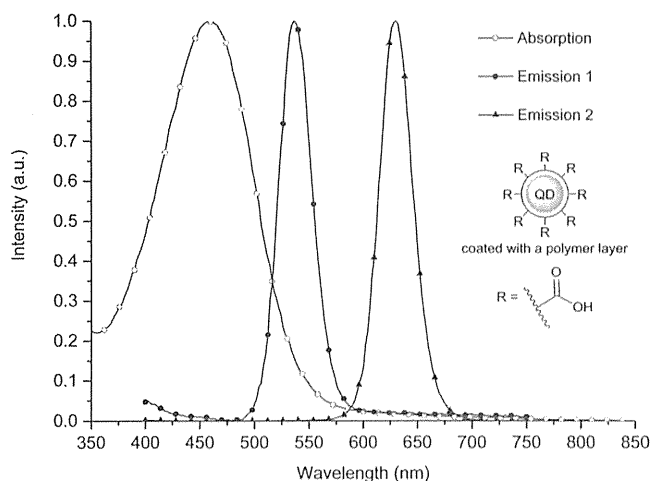


Figure 10. Absorption of C_{27} -aldehyde 17 (○) and fluorescence of reaction with QD 525 (●) and QD 625 (▲) in DMSO ($\lambda_{ex} = 360$ nm).

synthesis of nanoparticles bound to plant volatile precursors. Although it would be most desirable to use purified conjugates for the *in vivo* visualization of the formation of carotenoid-derived plant volatiles, the findings of this study suggest that the reaction mixtures containing freshly generated QD conjugate-1 should be sufficient for elucidating the primary and secondary metabolic pathways in plants in the future. Moreover, multicolor fluorescence imaging may be possible using QDs of different sizes, bound to the precursors, intermediates, and enzymes. This approach can be applied to study the localization, transport, storage, and crosstalk between the diverse and complex biosynthesis pathways utilizing distinct QDs for the staining of precursors, reaction products, and enzymes. Additional information on the enzymatic reaction will be reported elsewhere in due course.

EXPERIMENTAL SECTION

Synthesis of C_{10} -Triphenylphosphonium Ylide 5. (*E*)-3,5,5-Trimethyl-4-(2-(2-methyl-1,3-dioxolan-2-yl)vinyl)cyclohex-2-en-1-one (**10**). Freshly distilled α -ionone (**6**, 1.92 g, 10 mmol) was transferred into a 50 mL round-bottom flask with hexane (1 mL) and was treated with ethylene glycol (1.86 g, 30 mmol). *p*-Toluene sulfonic acid monohydrate (29 mg, 0.15 mmol) was added, and the mixture was stirred at rt under Ar overnight. The product was partitioned between water and hexane, and the organic layer was washed with water (3×80 mL), dried over Na_2SO_4 , and evaporated to dryness to yield the crude acetal **9** (2.66 g) as a pale-yellow oil. The crude product was used in the next step without purification. The crude acetal **9** was transferred into a two-necked flask using acetonitrile (9.5 mL). K_2CO_3 (166 g, 1.2 mmol) was added, and the mixture was cooled down in an ice-salt bath to 0 °C under Ar. A 70% solution of *tert*-butyl hydroperoxide (TBHP) in water (10.7 mL, TBHP: 75 mmol) was added dropwise to the mixture under Ar at 0 °C in 30 min. House bleach containing 5.25% NaOCl (49.6 g, NaOCl: 35 mmol) was then added over a period of 5 h at -10 to 0 °C. After the addition was completed, the reaction mixture was stirred at 0 °C for an additional hour. The product was treated with $NaHCO_3$ (185 mg) at 0 °C and then extracted with hexane. The combined organic layer was dried over Na_2SO_4 , and evaporated to dryness to give the crude product (2.58 g). The crude product was purified by autocolumned chromatography (hexane/ethyl acetate = 70:30) to yield the enone **10** (765 mg, 40% over two steps) as a pale-yellow oil. Registry no. 79709-34-5; 1H NMR (300 MHz, $CDCl_3$) δ 5.87 (s, 1H), 5.68 (dd, $J = 15.4$, 9.2 Hz, 1H), 5.53 (d, $J = 15.4$ Hz, 1H), 4.01–3.75 (m, 4H), 2.51 (d, $J = 9.2$ Hz, 1H), 2.30 (d, $J = 16.7$ Hz, 1H), 2.05 (d, $J = 16.7$ Hz, 1H),

1.85 (d, $J = 1.3$ Hz, 3H), 1.43 (s, 3H), 0.99 (s, 3H), 0.92 (s, 3H); ^{13}C NMR (75 MHz, $CDCl_3$) δ 199.1 (C=O), 161.4 (C), 135.0 (CH), 127.7 (CH), 126.0 (CH), 107.0 (C), 64.5 (CH₂), 54.9 (CH), 47.5 (CH₂), 36.0 (C), 27.7 (CH₃), 26.9 (CH₃), 25.0 (CH₃), 23.3 (CH₃).

(*E*)-4-(4-Hydroxy-2,6,6-trimethylcyclohex-2-en-1-yl)but-3-en-2-one (**12**). A solution of the enone **10** (50 mg, 0.2 mmol) in CH_2Cl_2 (0.36 mL) was cooled down to -30 °C under Ar, and a solution of DIBAL (0.36 mL of 1 M in hexane, 0.36 mmol) was added with a syringe in 5 min. The mixture was stirred at -30 °C to -20 °C for 1 h. The reaction was quenched by adding water at -10 °C followed by silica gel (0.25 g). The mixture was filtered through Celite, and CH_2Cl_2 was removed *in vacuo*. The residue was dissolved in acetone (0.5 mL) and water (0.26 mL), and 0.3 M HCl (20 μ L) was added. The mixture was stirred at rt for 30 min and extracted with ethyl acetate. The combined organic layer was dried over Na_2SO_4 and evaporated to dryness to give the crude product. The crude product was purified by column chromatography (hexane/ethyl acetate = 60:40) to give a mixture of *trans*- and *cis*-enone **12** (38 mg, 91%) in *trans/cis* diastereometric ratio of 33:67.

(*E*)-4-((1*R**,4*R**)-4-Hydroxy-2,6,6-trimethylcyclohex-2-en-1-yl)-but-3-en-2-one (*trans*-**12**): Registry no. 118015-38-6; 1H NMR (300 MHz, $CDCl_3$) δ 6.55 (dd, $J = 15.8$, 10.2 Hz, 1H), 6.11 (d, $J = 15.8$ Hz, 1H), 5.63 (brs, 1H), 4.38–4.19 (m, 1H), 2.51 (d, $J = 10.2$ Hz, 1H), 2.27 (s, 3H), 2.13 (brs, 1H), 1.84 (dd, $J = 13.4$, 5.9 Hz, 1H), 1.62 (s, 3H), 1.41 (dd, $J = 13.4$, 6.6 Hz, 1H), 1.03 (s, 3H), 0.89 (s, 3H); ^{13}C NMR (75 MHz, $CDCl_3$) δ 198.2 (C=O), 147.3 (CH), 135.1 (C), 133.6 (CH), 126.0 (CH), 65.1 (CH), 54.1 (CH), 43.7 (CH₂), 33.7 (C), 29.1 (CH₃), 26.9 (CH₃), 24.3 (CH₃), 22.4 (CH₃).

(*E*)-4-((1*S**,4*R**)-4-Hydroxy-2,6,6-trimethylcyclohex-2-en-1-yl)-but-3-en-2-one (*cis*-**12**): Registry no. 118015-37-5; 1H NMR (300 MHz, $CDCl_3$) δ 6.63 (dd, $J = 15.8$, 9.6 Hz, 1H), 6.08 (d, $J = 15.8$ Hz, 1H), 5.59 (s, 1H), 4.32–4.20 (m, 1H), 2.28 (d, $J = 9.6$ Hz, 1H), 2.26 (s, 3H), 1.70 (dd, $J = 13.0$, 6.5 Hz, 1H), 1.63 (t, $J = 1.6$ Hz, 3H), 1.59 (brs, 1H), 1.39 (dd, $J = 13.0$, 9.8 Hz, 1H), 0.98 (s, 3H), 0.89 (s, 3H); ^{13}C NMR (75 MHz, $CDCl_3$) δ 198.5 (C=O), 147.8 (CH), 135.5 (C), 132.8 (CH), 126.5 (CH), 66.4 (CH), 54.3 (CH), 40.6 (CH₂), 34.9 (C), 29.0 (CH₃), 27.0 (CH₃), 26.9 (CH₃), 22.3 (CH₃).

(*E*)-4-(4-Hydroxy-2,6,6-trimethylcyclohex-1-en-1-yl)but-3-en-2-one (**13**). A solution of *trans*-enone **12** (52 mg, 0.25 mmol) in THF (0.2 mL) was treated with a solution of KOH in methanol (10 wt %/v, 14 μ L) under Ar. The mixture was heated to 50 °C for 1.5 h, and the product was partitioned between water and ethyl acetate. The organic layer was washed with water, dried over Na_2SO_4 , and evaporated to dryness to give the crude product (84 mg). The crude product was purified by column chromatography to give the 3-hydroxy- β -ionone **13** (42 mg, 81% yield) as a yellow oil. Registry no. 116296-75-4; 1H NMR (300 MHz, $CDCl_3$) δ 7.22 (d, $J = 16.4$ Hz, 1H), 6.12 (d, $J = 16.4$ Hz, 1H), 4.10–3.89 (m, 1H), 2.44 (dd, $J = 17.4$, 5.4 Hz, 1H), 2.31 (s, 3H), 2.10 (dd, $J = 18.2$, 10.2 Hz, 1H), 1.99 (brs, 1H), 1.85–1.78 (m, 1H), 1.78 (s, 3H), 1.12 (s, 3H), 1.11 (s, 3H); ^{13}C NMR (75 MHz, $CDCl_3$) δ 198.7 (C=O), 142.4 (CH), 135.7 (C), 132.4 (C), 132.3 (CH), 64.3 (CH), 48.3 (CH₂), 42.7 (CH₂), 36.8 (C), 29.9 (CH₃), 28.4 (CH₃), 27.1 (CH₃), 21.4 (CH₃).

((2*E*,4*E*)-5-(4-Hydroxy-2,6,6-trimethylcyclohex-1-en-1-yl)-3-methylpenta-2,4-dien-1-yl)triphenylphosphonium Bromide (**5**). A solution of the 3-hydroxy- β -ionone **13** (54 mg, 0.26 mmol) in toluene (1.0 mL) was cooled down to -20 °C under Ar. A 1 M solution of vinyl magnesium bromide (0.63 mL, 0.63 mmol) was added dropwise in 10 min, and the mixture was stirred at -20 °C for 2 h. The reaction was quenched with addition of saturated ammonium chloride solution at -20 °C and stirred at rt for 10 min. The reaction mixture was partitioned between water and ethyl acetate. The organic layer was washed with water, dried over Na_2SO_4 , and evaporated to dryness. The crude tertiary vinyl- β -ionol **14** was dissolved in MeOH (0.3 mL) and directly used in the next step for the preparation of the Wittig salt **5**. Triphenylphosphine hydrobromide (1.72 g, 5 mmol) was added to methanol (0.3 mL) at 0 °C. The solution was stirred at rt for 20 min and then treated with a solution of the crude tertiary vinyl- β -ionol **14** in MeOH (0.3 mL) by dropwise addition at 0 °C. The reaction was kept at 0 °C for 1 h and was allowed to stir to rt overnight. The

product was partitioned between hexane (5 mL) and methanol–water (1:1 v/v, 5 mL). The aqueous layer was washed with hexane to remove the excess triphenylphosphine hydrobromide, and the aqueous layer was extracted with CH₂Cl₂. The combined CH₂Cl₂ layer was washed with water, dried over Na₂SO₄, and evaporated to dryness to give the C₁₅-phosphonium ylide **5** that was used directly to prepare the C₂₅-aldehyde **4** without purification.

Synthesis of C₁₀-Dialdehyde 7. Tetraethyl But-2-ene-1,4-diyl (E)-Bis(phosphonate) (15). Triethyl phosphite (0.53 g, 3.2 mmol) and (E)-1,4-dichlorobut-2-ene (**8**, 125 mg, 1.0 mmol) were added to an autoclave under Ar. The reaction was carried out under 0.4 MPa, 160 °C over 2 h. After removing the excess reagent by distillation at 160 °C under 2.6 mmHg, the phosphonate **15** (301 mg, 92%) was obtained as the dark-orange residue. Registry no. 16626-80-5; ¹H NMR (300 MHz, CDCl₃) δ 5.62 (brs, 2H), 4.24–3.97 (m, 8H), 2.61 (dd, *J* = 17.5, 4.1 Hz, 4H), 1.32 (t, *J* = 7.0 Hz, 12H); ¹³C NMR (75 MHz, CDCl₃) δ 124.3 (d, *J* = 3.8 Hz, CH), 61.7 (CH₂), 31.3 (d, *J* = 3.9 Hz, CH₂), 29.4 (d, *J* = 3.9 Hz, CH₂), 16.2 (CH₃).

(2E,4E,6E)-2,7-Dimethylocta-2,4,6-trienedial (7). Dispersion of sodium hydride (60% dispersion, 64 mg, 1.6 mmol) in anhydrous THF (0.80 mL) was cooled in ice bath under Ar. A solution of the phosphonate **15** (66 mg, 0.2 mmol) dissolved in anhydrous THF (0.8 mL) was then added. The mixture was allowed to stir for 15 min. A solution of 1,1-dimethoxypropan-2-one (118 mg, 1.0 mmol) in anhydrous THF (0.40 mL) was added dropwise. The reaction mixture was carried out under reflux condition. It was observed that the solution changed color from colorless to light yellow. After 3.5 h, 20% sulfuric acid (0.3 mL) was added at 0 °C, increasing the reaction temperature to 50 °C over 2.5 h. The reaction mixture was extracted with diethyl ether. The combined organic layer was dried over Na₂SO₄, concentrated *in vacuo*, and purified by column chromatography (hexane/AcOEt = 100:0 to 80:20) to yield the C₁₀-dialdehyde **7** (11 mg, y. 35%) as a yellow solid. Registry no. 5056-17-7; ¹H NMR (300 MHz, CDCl₃) δ 9.55 (s, 2H), 7.13–6.95 (m, 4H), 1.95 (s, 6H); ¹³C NMR (75 MHz, CDCl₃) δ 194.5 (C=O), 146.08 (CH), 141.1 (C), 134.4 (CH), 9.7 (CH₃).

Synthesis of C₂₇-Aldehyde 17. (2E,4E,6E,8E,10E,12E)-13-(4-Hydroxy-2,6,6-trimethylcyclohex-1-en-1-yl)-2,7,11-trimethyltrideca-2,4,6,8,10,12-hexaenal (4). A mixture of the crude C₁₅-phosphonium ylide **5** (209 mg, 0.37 mmol) and the C₁₀-dialdehyde **7** (51 mg, 0.31 mmol) and 1,2-epoxybutane (0.56 mL) in ethanol (5.6 mL) was refluxed under Ar. The reaction was carried out overnight. The reaction mixture was then diluted with water (10 mL) and extracted with diethyl ether (3 × 5 mL). The organic layer was dried over Na₂SO₄, and the solvent was removed *in vacuo*. The crude product was purified by autocolumn chromatography to give the C₂₅-aldehyde **4** (53.4 mg, 56% yield over three steps). Registry no. 50837-94-0; ¹H NMR (300 MHz, CDCl₃) δ 9.42 (s, 1H), 7.10–6.84 (m, 2H), 6.84–6.54 (m, 2H), 6.45–6.21 (m, 2H), 6.20–6.05 (m, 3H), 4.04–3.87 (m, 1H), 2.36 (dd, *J* = 16.8, 4.6 Hz, 1H), 2.14–1.70 (m, 2H), 2.01 (s, 3H), 1.99 (s, 1H), 1.96 (s, 3H), 1.85 (s, 3H), 1.71 (s, 3H), 1.46 (t, *J* = 11.9 Hz, 1H), 1.05 (s, 6H); ¹³C NMR (75 MHz, CDCl₃) δ 194.5 (C=O), 149.0 (CH), 141.7 (C), 138.2 (CH), 137.8 (CH), 137.6 (C), 137.6 (C), 136.8 (C), 136.6 (CH), 131.0 (CH), 130.8 (CH), 127.5 (CH), 127.4 (CH), 126.8 (CH), 126.7 (C), 64.8 (CH), 48.2 (CH₂), 42.4 (CH₂), 36.9 (C), 30.1 (CH₃), 28.6 (CH₃), 21.4 (CH₃), 12.9 (CH₃), 12.6 (CH₃), 9.4 (CH₃).

Ethyl (2E,4E,6E,8E,10E,12E,14E)-15-(4-Hydroxy-2,6,6-trimethylcyclohex-1-en-1-yl)-4,9,13-trimethylpentadeca-2,4,6,8,10,12,14-heptaenoate (16). A solution of ethyl (triphenylphosphoranylidene)-acetate (21 mg, 0.06 mmol) and the C₂₅-aldehyde **4** (7.3 mg, 0.02 mmol) in dry THF (0.25 mL) was heated at 95 °C for 7 h in a sealed tube. The reaction mixture was cooled to room temperature and diluted with water and Et₂O. Phases were separated, and the aqueous phase was extracted with Et₂O. The combined organic layer was dried over Na₂SO₄, filtered and concentrated *in vacuo*. The crude product was purified by autochromatography (hexane/ethyl acetate = 95:5) to yield the ester **16** (5.1 mg, 35%). The coupling constant for the newly formed double bond confirms the *E* stereochemistry by ¹H NMR spectroscopy. Registry no. unknown; ¹H NMR (300 MHz, CDCl₃) δ

7.38 (d, *J* = 15.5 Hz, 1H), 7.00–6.44 (m, 4H), 6.43–6.04 (m, 5H), 5.88 (d, *J* = 15.5 Hz, 1H), 4.22 (q, *J* = 7.1 Hz, 2H), 4.11–3.90 (m, 1H), 2.39 (dd, *J* = 16.4, 4.9 Hz, 1H), 2.14–1.65 (m, 3H), 2.00 (s, 3H), 1.98 (s, 3H), 1.92 (s, 3H), 1.74 (s, 3H), 1.47 (t, *J* = 12.0 Hz, 1H), 1.31 (t, *J* = 7.1 Hz, 3H), 1.07 (s, 6H); ¹³C NMR (75 MHz, CDCl₃) δ 167.6 (C=O), 148.8 (CH), 139.3 (CH), 138.9 (C), 138.4 (CH), 137.7 (C), 137.2 (CH), 136.6 (C), 133.8 (CH), 133.6 (C), 131.9 (CH), 131.1 (CH), 128.8 (CH), 126.4 (C), 126.2 (2 × CH), 116.4 (CH), 65.0 (CH), 60.1 (CH₂), 48.3 (CH₂), 42.5 (CH₂), 37.0 (C), 30.2 (CH₃), 28.6 (CH₃), 21.5 (CH₃), 14.2 (CH₃), 12.8 (CH₃), 12.7 (CH₃), 12.4 (CH₃); ESI-TOF high resolution mass: calcd for C₂₉H₄₁O₃ [M + H]⁺ 437.3056, found 437.3054.

(2E,4E,6E,8E,10E,12E,14E)-15-(4-Hydroxy-2,6,6-trimethylcyclohex-1-en-1-yl)-4,9,13-trimethylpentadeca-2,4,6,8,10,12,14-heptaenal (17). To a cold solution of the ester **16** (5.1 mg, 12 μmol) in anhydrous Et₂O (0.2 mL) was added DIBAL (1 M solution in hexane, 50 μL, 50 μmol) at 0 °C and stirred for 20 min. Roschell salt was added, and glycerol (3 drops) were added for quenching. The reaction mixture was stirred 2 h at rt. Phases were separated, and the aqueous phase was extracted with Et₂O. The combined organic layers were washed with brine, dried over Na₂SO₄, filtered, and concentrated *in vacuo* to give the corresponding allylic alcohol, which was used without further purification. MnO₂ (10 mg, 0.12 mmol) was added to a stirred solution of the above allylic alcohol in CH₂Cl₂ (3 mL) at 0 °C and stirred for 3.5 h. The reaction mixture was filtered through a pad of Celite and washed with CH₂Cl₂. Solvent was removed *in vacuo*, and the crude aldehyde was purified by auto silica column chromatography to yield the C₂₇-aldehyde **17** (2.0 mg, 44%). Registry no. 15486-31-4; ¹H NMR (300 MHz, CDCl₃) δ 9.57 (d, *J* = 7.8 Hz, 1H), 7.15 (d, *J* = 15.4 Hz, 1H), 7.06–6.49 (m, 4H), 6.42–6.05 (m, 6H), 4.05–3.88 (m, 1H), 2.38 (dd, *J* = 17.0, 5.5 Hz, 1H), 2.14–1.70 (m, 3H), 2.00 (s, 3H), 1.97 (s, 3H), 1.94 (s, 3H), 1.72 (s, 3H), 1.47 (t, *J* = 11.92 Hz, 1H), 1.06 (s, 6H); ¹³C NMR (75 MHz, CDCl₃) δ 193.8 (C=O), 156.7 (CH), 141.2 (CH), 140.0 (C), 138.3 (CH), 137.7 (C), 137.1 (C), 137.0 (CH), 135.3 (CH), 133.7 (C), 131.7 (CH), 131.0 (CH), 128.5 (CH), 127.1 (CH), 126.8 (CH), 126.6 (C), 126.5 (CH), 64.9 (CH), 48.3 (CH₂), 42.4 (CH₂), 37.0 (C), 30.1 (CH₃), 28.6 (CH₃), 21.5 (CH₃), 12.8 (CH₃), 12.7 (CH₃), 12.5 (CH₃).

Coupling Reaction between QDs and the C₂₇-Aldehyde 17.

To a colloidal solution of QDs (1 mM, 20 μL, 20 nmol) in 2-(*N*-morpholino)ethanesulfonic acid (MES) buffer was added 1-ethyl-3-(3-(dimethylamino)propyl)carbodiimide hydrochloride (10 μg/μL in MES, 385 μL, 20 μmol) and *N*-hydroxysuccinimide (NHS, 10 μg/μL in MES, 230 μL, 20 μmol) in MES buffer. The reaction mixture was stirred for 15 min. The reaction solution was treated with a solution of the C₂₇-aldehyde **17** (785 μL in DMF, 1 μg/μL, 2 μmol) and stirred overnight. Absorption and fluorescence spectra of the reaction mixture were subsequently measured over the time.

■ ASSOCIATED CONTENT

📄 Supporting Information

The experimental details, and the copies of NMR spectra. This material is available free of charge via the Internet at <http://pubs.acs.org>.

■ AUTHOR INFORMATION

Corresponding Authors

*E-mail: tnmase@ipc.shizuoka.ac.jp (N.M.)

*E-mail: Baldermann@igzev.de (S.B.)

Notes

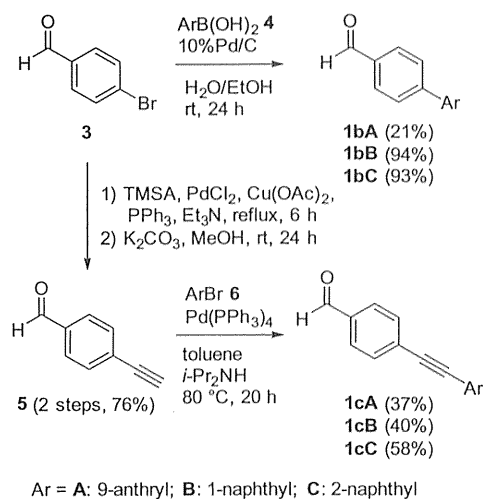
The authors declare no competing financial interest.

■ ACKNOWLEDGMENTS

This study was supported in part by Nanobio Project from Shizuoka University.

■ REFERENCES

- (1) Auldridge, M. E.; McCarty, D. R.; Klee, H. J. *Curr. Opin. Plant Biol.* **2006**, *9*, 315–321.
- (2) Young, A. J.; Frank, H. A. J. *Photochem. Photobiol., B* **1996**, *36*, 3–15.
- (3) Simkin, A. J.; Schwartz, S. H.; Auldridge, M.; Taylor, M. G.; Klee, H. J. *Plant J.* **2004**, *40*, 882–892.
- (4) Knudsen, J. T.; Eriksson, R.; Gershenzon, J.; Ståhl, B. *Bot. Rev.* **2006**, *72*, 1–120.
- (5) Cooper, C. M.; Davies, N. W.; Menary, R. C. *J. Agric. Food Chem.* **2003**, *51*, 2384–2389.
- (6) Han, Y.; Li, L.; Dong, M.; Yuan, W.; Shang, F. *Biologia* **2013**, *68*, 258–263.
- (7) Zhu, M.; Li, E.; He, H. *Chromatographia* **2008**, *68*, 603–610.
- (8) Reviews on the conjugation of biomolecules to QDs: (a) Blanco-Canosa, J. B.; Wu, M.; Susumu, K.; Petryayeva, E.; Jennings, T. L.; Dawson, P. E.; Algar, W. R.; Medintz, I. L. *Coord. Chem. Rev.* **2014**, *263*, 101–137. (b) Esteve-Turrillas, F. A.; Abad-Fuentes, A. *Biosens. Bioelectron.* **2013**, *41*, 12–29. (c) Li, J.; Wu, D.; Miao, Z.; Zhang, Y. *Curr. Pharm. Biotechnol.* **2010**, *11*, 662–671. (d) Resch-Genger, U.; Grabolle, M.; Cavaliere-Jaricot, S.; Nitschke, R.; Nann, T. *Nat. Methods* **2008**, *5*, 763–775 and references cited therein.
- (9) (a) Khachik, F.; Chang, A.-N. *Synthesis* **2011**, 509–516. (b) Ellis, P. R.; Faruk, A. E.; Moss, G. P.; Weedon, B. C. L. *Helv. Chim. Acta* **1981**, *64*, 1092–1097. (c) Ito, M.; Matsuoka, N.; Tsukida, K.; Seki, T. *Chem. Pharm. Bull.* **1988**, *36*, 78–86.
- (10) Kauffman, J. M.; Moyna, G. J. *Org. Chem.* **2003**, *68*, 839–853.
- (11) Details of QDs: QD 510, 620 carboxyl (EMFUTUR technologies CdTe QD 510 or 620 nm), in which the core is prepared from CdTe, which is commercially available, hydrophilic, and has a terminal –COOH group. According to the supplier's information (EMFUTUR technologies), the molar weights of these nanocrystals are about 3000 for QD 510 and 90,000 for QD 620. They easily form colloidal particles in distilled or deionized water. The spherical particles are coated with proprietary low-molecular weight thiocarboxylic acid residues (HS-R-COOH). The largest ligand R = (CH₂)₃ makes the total length (<1 nm) small enough to enable a highly efficient FRET. The approximate density of –COOH groups on the surface of quantum dots is 5–6 groups per square nanometer.
- (12) Wang, S.; Mamedova, N.; Kotov, N. A.; Chen, W.; Studer, J. *Nano Lett.* **2002**, *2*, 817–822.
- (13) Details of QDs: Qdot ITK (Innovator's Tool Kit, Invitrogen) 525, 625 carboxyl quantum dots are commercially available and prepared from nanometer-scale crystals of a semiconductor material (CdSe), which are shelled with an additional semiconductor layer (ZnS) to improve their chemical and optical properties. According to the supplier's information (Life Technologies), the core-shell materials are further coated with a polymer layer that allows the facile dispersion of the quantum dots in aqueous solutions with retention of their optical properties. The polymer coating has –COOH surface groups available for modifications such as macromolecule attachment. Qdot ITK carboxyl quantum dots are about the size of large macromolecules or proteins.

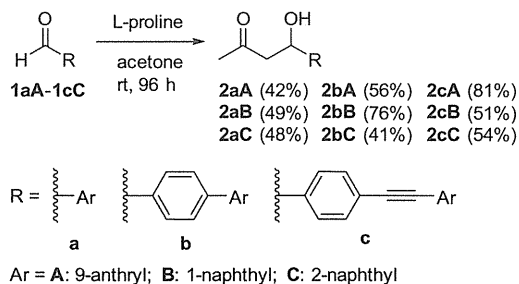


Scheme 2. Preparation of benzaldehyde derivatives 1.

The syntheses of 4-arylbenzaldehyde derivatives **1b** and 4-arylethynylbenzaldehyde derivatives **1c** are shown in Scheme 2. The Pd/C-catalyzed phosphine-free Suzuki–Miyaura reactions¹² of 4-bromobenzaldehyde (**3**) and boronic acids **4** at room temperature afforded the 4-arylbenzaldehyde derivatives **1bA–1bC** in moderate to excellent (21–94%) yields (Scheme 2). 4-Ethynylbenzaldehyde (**5**) was synthesized from **3** and trimethylsilylacetylene (TMSA) in 76% yield over two steps.¹³ The Sonogashira coupling reactions¹⁴ of aldehyde **5** and aryl bromides **6** at 80 °C afforded the corresponding aldehydes **1cA–1cC** in moderate to good (37–58%) yields.

Aldols **2** were prepared by the organocatalytic L-proline-catalyzed aldol reactions¹⁵ between acetone and benzaldehyde derivatives **1** (Scheme 3). Nine derivatives **2aA–2cC** were prepared in moderate to good (41–81%) yields at room temperature without any special operation.

First, aldehydes **1aA–1aC** were evaluated. 9-Anthraldehyde (**1aA**) emits very weak fluorescence in many solvents upon UV irradiation at the appropriate wavelengths;¹⁶ whereas, it is known that anthracen-9-ylmethanol emits strong blue fluorescence.¹⁷ Similarly, aldol **2aA** was highly fluorescent in DMSO.^{7c} The ratio of the fluorescence intensities of **2aA** to **1aA** was 322 in DMSO (Table 1, entry 1). To test the utility of **1aA** for monitoring the reaction progress of a typical organocatalytic aldol reaction, the reaction between acetone and aldehyde **1aA** was performed using L-proline as the catalyst, and the fluorescence intensity was recorded (Fig. 1, see also the Supplementary Material for the details of the fluorescence spectra). Although aldol **2aA** was highly fluorescent, the increase in the fluorescence intensity observed during the reaction was low; the slope over 1 h was 0.09. The L-proline-catalyzed aldol reaction of aldehyde **1aA** with acetone



Scheme 3. Organocatalytic aldol reactions of benzaldehyde derivatives 1.

Table 1
Fluorescent properties of aryl aldehyde derivatives **1** and the corresponding aldols **2**

Entry	Wavelength (nm)		Fluorescence intensity			Fold	
	λ_{ex}	λ_{em}	Aldehyde 1		Aldol 2		
1	265	419	1aA	1.66×10^1	2aA	5.34×10^3	322
2	220	—	1aB	—	2aB	—	—
3	235	—	1aC	—	2aC	—	—
4	265	401	1bA	4.17×10^1	2bA	2.49×10^3	60
5	300	342	1bB	5.66×10^1	2bB	2.63×10^2	4.6
6	270	363	1bC	8.51×10^1	2bC	1.33×10^3	16
7	270	432	1cA	6.16×10^1	2cA	8.21×10^3	133
8	330	351	1cB	2.08×10^1	2cB	7.65×10^3	368
9	330	347	1cC	2.12×10^1	2cC	6.42×10^3	303

All measurements were carried out in 1.0 μ M DMSO solution.

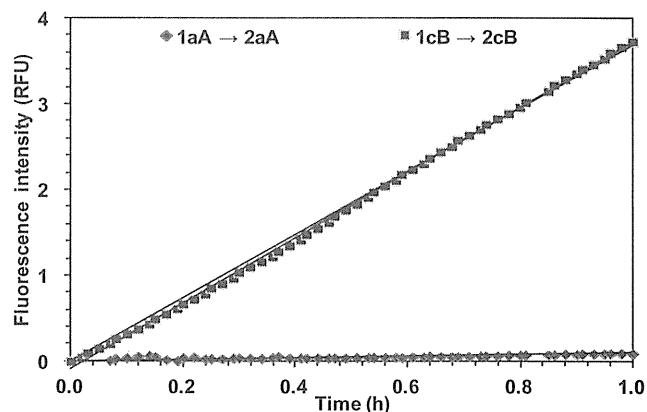
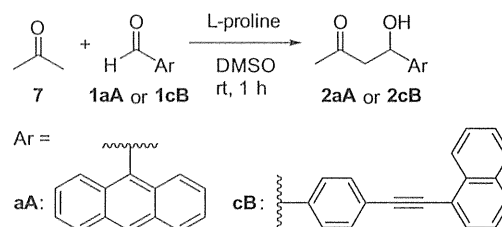


Figure 1. Fluorescence monitoring of aldol reactions; reaction conditions: aldehyde (10 μ M), L-proline (1 mM) in 20% acetone/75% DMSO/5% H₂O; reaction volume 3 mL; the reaction was performed in a quartz cuvette. For the reaction of **1aA** with acetone, the fluorescence intensity of **2aA** was monitored at λ_{ex} = 265 nm and λ_{em} = 420 nm; the slope over 1 h was 0.09. For the reaction of **1cB** with acetone, the fluorescence intensity of **2cB** was monitored at λ_{ex} = 330 nm and λ_{em} = 351 nm; the slope over 1 h was 3.68.

to afford **2aA** was too slow to obtain any reasonable data. The bulkiness of the 9-anthryl group probably caused the slow reaction. When less bulky naphthalene derivatives **1aB/2aB** and **1aC/2aC** were evaluated, no fluorescence was observed at 1 μ M concentration in DMSO under the UV irradiation at 220 and 235 nm, respectively (Table 1, entries 2 and 3). Although naphthalene derivatives are known to be fluorescent,¹⁸ the results of the fluorescence measurements of **1aB/2aB** and **1aC/2aC** in DMSO indicate that naphthaldehydes are not good fluorogenic substrates for the analysis of the formation of the aldols at the initial stages of the reactions.

Next, arylbenzene derivatives **1b** and arylolethynylbenzene derivatives **1c** were evaluated. Aldehydes **1bA–1bC** and **1cA–1cC** emitted very weak fluorescence, whereas aldols **2bA–2bC** and **2cA–2cC** emitted strong fluorescence in DMSO under the irradiation at appropriate wavelengths (Table 1, entries 4–9). The ratios of the fluorescence intensities of **2b/1b** varied from 4.6 to 60 (Table 1, entries 4–6), whereas those of **2c/1c** were more than 100 (Table 1, entries 7–9). The best pair of aldol/aldehyde among

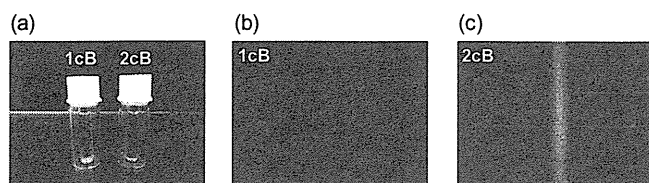


Figure 2. Photographs of the solutions of 1-naphthylethynylbenzene derivatives in DMSO (0.1 mM): (a) aldehyde **1cB** and aldol **2cB** under visible light; (b) aldehyde **1cB** and (c) aldol **2cB** under UV light at $\lambda_{\text{ex}} = 254$ nm (UV lamp), $\lambda_{\text{em}} = 300$ –400 nm (UV camera with filters BLF-390B and UTVAF-50S-33U, Sigma Koki Co., Ltd, Japan).

those tested was **2cB/1cB** with a fluorescence intensity ratio of 368 (Table 1, entry 8).¹⁹ The UV light images of aldehyde **1cB** and aldol **2cB** clearly show the OFF–ON property of the pair (Fig. 2).

Aldehyde **1cB** showed the lowest fluorescence among aldehydes **1bA–1bC** and **1cA–1cC**; therefore, the utility of aldehyde **1cB** in monitoring the reaction to afford aldol **2cB** was examined. The time course of the L-proline-catalyzed aldol reaction of acetone with aldehyde **1cB** showed a significant increase in the fluorescence intensity (Fig. 1); the slope over 1 h was 3.68. This slope was 41-fold greater than that of the L-proline-catalyzed reaction of **1aA** with acetone to afford aldol **2aA**. These results indicate that aldehyde **1cB** is an excellent fluorogenic aldehyde for monitoring the reaction progress of aldol reactions in DMSO.

In summary, we developed fluorogenic aldehydes that can be used to monitor the reaction progress of L-proline-catalyzed aldol reactions in DMSO through an increase in the fluorescence intensity. This type of fluorescence assay system may be useful for the rapid identification of superior aldol catalysts. The studies on the full scope of the fluorescence monitoring systems for chemical transformations using fluorogenic substrates containing arylolethynylbenzene moieties are currently under investigation and will be reported in due course.

Acknowledgments

This study was supported in part by a Grant-in-Aid for Young Scientists (A) (No. 23685035) for scientific research from the Japan Society for the Promotion of Science.

Supplementary data

Supplementary data associated with this article can be found, in the online version, at <http://dx.doi.org/10.1016/j.tetlet.2014.02.007>.

References and notes

- Reviews on fluorogenic substrates: (a) Finney, N. S. *Curr. Opin. Chem. Biol.* **2006**, *10*, 238–245; (b) Goddard, J.-P.; Raymond, J.-L. *Trends Biotechnol.* **2004**, *22*, 363–370; (c) Evans, C. A.; Miller, S. J. *Curr. Opin. Chem. Biol.* **2002**, *6*, 333–338.
- Recent reports on the detection of bond-cleavage reactions in enzyme assay: (a) Baba, R.; Hori, Y.; Mizukami, S.; Kikuchi, K. *J. Am. Chem. Soc.* **2012**, *134*, 14310–14313; (b) Kumada, H.-O.; Nguyen, J.-T.; Kakizawa, T.; Hidaka, K.; Kimura, T.; Hayashi, Y.; Kiso, Y. *J. Pept. Sci.* **2011**, *17*, 569–575; (c) Sicart, R.; Collin, M.-P.; Raymond, J.-L. *Biotechnol. J.* **2007**, *2*, 221–231.
- Recent reports on the detection of bond-cleavage reactions: (a) Shibata, A.; Furukawa, K.; Abe, H.; Tsuneda, S.; Ito, Y. *Bioorg. Med. Chem. Lett.* **2008**, *18*, 2246–2249; (b) Yang, X.-F. *Spectrochim. Acta, Part A* **2007**, *67*, 321–326; (c) Wu, J.-S.; Kim, H. J.; Lee, M. H.; Yoon, J. H.; Lee, J. H.; Kim, J. S. *Tetrahedron Lett.* **2007**, *48*, 3159–3162.
- Recent reports on the detection of C–C bond-cleavage reactions: (a) Sevestre, A.; Charmantray, F.; Hélaine, V.; Lásiková, A.; Hecquet, L. *Tetrahedron* **2006**, *62*, 3969–3976; (b) Kofoed, J.; Darbre, T.; Raymond, J.-L. *Org. Biomol. Chem.* **2006**, *4*, 3268–3281; (c) Jourdain, N.; Carlón, R. P.; Raymond, J.-L. *Tetrahedron Lett.* **1998**, *39*, 9415–9418; (d) List, B.; Barbas, C. F., III; Lerner, R. A. *Proc. Natl. Acad. Sci. U. S. A.* **1998**, *95*, 15351–15355.
- Recently reported fluorogenic probes for bond-forming chemical transformations and detecting molecules of interest by covalent bond-forming reactions: (a) Mizukami, S.; Watanabe, S.; Akimoto, Y.; Kikuchi, K. *J. Am. Chem. Soc.* **2012**, *134*, 1623–1629; (b) Lang, K.; Davis, L.; Wallace, S.; Mahesh, M.; Cox, D. J.; Blackman, M. L.; Fox, J. M.; Chin, J. W. *J. Am. Chem. Soc.* **2012**, *134*, 10317–10320; (c) Shieh, P.; Hangauer, M. J.; Bertozzi, C. R. *J. Am. Chem. Soc.* **2012**, *134*, 17428–17431; (d) Friscourt, F.; Fahrni, C. J.; Boons, G.-J. *J. Am. Chem. Soc.* **2012**, *134*, 18809–18815; (e) Zhang, H.; Wang, P.; Yang, Y.; Sun, H. *Chem. Commun.* **2012**, *48*, 10672–10674; (f) Komatsu, T.; Johansson, K.; Okuno, H.; Bito, H.; Inoue, T.; Nagano, T.; Urano, Y. *J. Am. Chem. Soc.* **2011**, *133*, 6745–6751; (g) Eor, S.; Hwang, J.; Choi, M. G.; Chang, S.-K. *Org. Lett.* **2011**, *13*, 370–373; (h) Jewett, J. C.; Bertozzi, C. R. *Org. Lett.* **2011**, *13*, 5937–5939; (i) Zhang, C.-J.; Li, L.; Chen, G. Y. J.; Xu, Q.-H.; Yao, S. Q. *Org. Lett.* **2011**, *13*, 4160–4163.
- Tanaka, F.; Thayumanavan, R.; Barbas, C. F., III *J. Am. Chem. Soc.* **2003**, *125*, 8523–8528.
- (a) Tanaka, F.; Mase, N.; Barbas, C. F., III *J. Am. Chem. Soc.* **2004**, *126*, 3692–3693; (b) Guo, H.-M.; Tanaka, F. *J. Org. Chem.* **2009**, *74*, 2417–2424; (c) Mase, N.; Takabe, K.; Tanaka, F. *Tetrahedron Lett.* **2013**, *54*, 4306–4308; (d) Katsuyama, I.; Chouthaiwale, P. V.; Akama, H.; Cui, H.-L.; Tanaka, F. *Tetrahedron Lett.* **2014**, *55*, 74–78.
- Guo, H.-M.; Minakawa, M.; Tanaka, F. *J. Org. Chem.* **2008**, *73*, 3964–3966.
- Recent reports on the detection of C–C bond-forming reactions: (a) Jo, J.; Olasz, A.; Chen, C.-H.; Lee, D. *J. Am. Chem. Soc.* **2013**, *135*, 3620–3632; (b) Sonawane, Y. A.; Phadtare, S. B.; Borse, B. N.; Jagtap, A. R.; Shankarling, G. S. *Org. Lett.* **2010**, *12*, 1456–1459; (c) Do, J. H.; Kim, H. N.; Yoon, J.; Kim, J. S.; Kim, H.-J. *Org. Lett.* **2010**, *12*, 932–934; (d) Kim, G.-J.; Kim, H.-J. *Tetrahedron Lett.* **2010**, *51*, 4670–4672; (e) Jo, J.; Lee, D. *J. Am. Chem. Soc.* **2009**, *131*, 16283–16291; (f) Zhao, D.; Wang, W.; Yang, F.; Lan, J.; Yang, L.; Gao, G.; You, J. *Angew. Chem., Int. Ed.* **2009**, *48*, 3296–3300; (g) Rozhkov, R. V.; Davisson, V. J.; Bergstrom, D. E. *Adv. Synth. Catal.* **2008**, *350*, 71–75; (h) Umeda, N.; Tsurugi, H.; Satoh, T.; Miura, M. *Angew. Chem., Int. Ed.* **2008**, *47*, 4019–4022.
- (a) Mase, N.; Tanaka, F.; Barbas, C. F., III *Org. Lett.* **2003**, *5*, 4369–4372; (b) Mase, N.; Tanaka, F.; Barbas, C. F., III *Angew. Chem., Int. Ed.* **2004**, *43*, 2420–2423; (c) Mase, N.; Thayumanavan, R.; Tanaka, F.; Barbas, C. F., III *Org. Chem., Int. Ed.* **2004**, *6*, 2527–2530; (d) Tanaka, F.; Thayumanavan, R.; Mase, N.; Barbas, C. F., III *Tetrahedron Lett.* **2004**, *45*, 325–328; (e) Tanaka, F.; Mase, N.; Barbas, C. F., III *Chem. Commun.* **2004**, 1762–1763.
- Katsuyama, I.; Chouthaiwale, P. V.; Cui, H.-L.; Ito, Y.; Sando, A.; Tokiwa, H.; Tanaka, F. *Tetrahedron* **2013**, *69*, 4098–4104.
- Zhang, G. *Synthesis* **2005**, 537–542.
- Wautelat, P.; Moigne, J. L.; Videva, V.; Turek, P. *J. Org. Chem.* **2003**, *68*, 8025–8036.
- Yi, C.; Hua, R. *Catal. Commun.* **2006**, *7*, 377–379.
- (a) List, B.; Lerner, R. A.; Barbas, C. F., III *J. Am. Chem. Soc.* **2000**, *122*, 2395–2396; (b) Sakthivel, K.; Notz, W.; Bui, T.; Barbas, C. F., III *J. Am. Chem. Soc.* **2001**, *123*, 5260–5267.
- (a) Crowell, E. P.; Varsel, C. *J. Anal. Chem.* **1963**, *35*, 189–192; (b) Mitchell, D. J.; Schuster, G. B.; Drickamer, H. G. *J. Am. Chem. Soc.* **1977**, *99*, 1145–1148.
- Vijayalakshmi, N.; Maitra, U. *Org. Lett.* **2005**, *7*, 2727–2730.
- (a) Liu, J.-F.; Chi, Y.-G.; Peng, J.-F.; Jiang, G.-B.; Jönsson, J. Å. *J. Chem. Eng. Data* **2004**, *49*, 1422–1424; (b) Kang, K.-D.; Jones, P. D.; Huang, H.; Zhang, R.; Mostovich, L. A.; Wheelock, C. E.; Watanabe, T.; Gulyaeva, L. F.; Hammock, B. D. *Anal. Biochem.* **2005**, *344*, 183–192.
- The ratios of the fluorescence intensities of 2cB/1cB in various solvents:** 232-fold in CHCl_3 (at $\lambda_{\text{ex}} = 320$ nm and $\lambda_{\text{em}} = 347$ nm), 323-fold in AcOEt (at $\lambda_{\text{ex}} = 318$ nm and $\lambda_{\text{em}} = 343$ nm), 22-fold in 2-PrOH (at $\lambda_{\text{ex}} = 318$ nm and $\lambda_{\text{em}} = 343$ nm), 764-fold in CH_3CN (at $\lambda_{\text{ex}} = 318$ nm and $\lambda_{\text{em}} = 343$ nm), 31-fold in DMF (at $\lambda_{\text{ex}} = 324$ nm and $\lambda_{\text{em}} = 347$ nm), and 15-fold in Na phosphate buffer (pH 7, at $\lambda_{\text{ex}} = 238$ nm and $\lambda_{\text{em}} = 360$ nm). The fluorescence intensity of aldol **2cB** in different solvents analyzed in the above-indicated λ_{ex} and λ_{em} wavelengths relative to that in DMSO (**2cB** in DMSO at $\lambda_{\text{ex}} = 330$ nm and $\lambda_{\text{em}} = 351$ nm: 100) was as follows: CHCl_3 : 97; AcOEt : 117; 2-PrOH: 121; CH_3CN : 119; DMF: 108; Na phosphate buffer (pH 7): 14.

